formed during the decomposition of terminal radicals. This would result in two types of "excess" methylene units: (i) $-OCH_2O_2-$ and (ii) $-SCH_2O_2-$. We find no peaks corresponding to the first type (ref 71). The second type would have a ^{13}C resonance in almost the same position as $\beta(O_2SS)$ resonances, although its presence was not detectable within experimental error on the basis of the equality between α and β backbone carbon resonance areas.
(54) The separation of the various peaks is too great to be due to configurational effects, which at most contribute only to a broadening of individual resonances.
(55) J. B. Stothers, "Carbon-13 NMR Spectroscopy", Academic Press, New York, N.Y., 1972, p 140.
(56) F. P. Price, "Markov Chains and Monte Carlo Calculations in Polymer Science", G. G. Lowry, Ed., Marcel Dekker, New York, N.Y., 1970, pp 199–201.
(57) K. Ito and Y. Yamashita, *J. Polym. Sci. A*, **3**, 2165–2187 (1965).
(58) The area of the O_2SO_2 peak is only 43% of that expected from the analysis of the backbone resonances, whereas the areas of the lower field quaternary resonances are in reasonable agreement. This discrepancy is due to a differential saturation of the O_2SO_2 resonance (pulse interval = 4.0 s, $T_1 >$ 3 s). The T_1's of quaternary carbons in sequences derived from SS dyads are not as long, due to an extra pair of neighboring methylene protons available for dipolar relaxation. Because of this differential saturation effect, we did not make quantitative use of the quaternary carbon O_2SO_2 resonance.
(59) It is unlikely that the resonances from the styrene unit removed from the end group by one peroxide unit will be noticeably perturbed in chemical shift from the positions of the main chain resonances, since at most only the γ substituent could vary with end-group structure. We therefore assume that all end-group resonances are due only to the carbons directly involved in this group.
(60) B. D. Coleman and T. G. Fox, *J. Polym. Sci. A*, **1**, 3183–3197 (1963).
(61) C. W. Pyun, *J. Polym. Sci., Part A-2*, **8**, 1111–1126 (1970).
(62) F. R. Mayo and F. M. Lewis, *J. Am. Chem. Soc.*, **66**, 1594–1601 (1944).
(63) The ^{13}C data were obtained with a pulse interval at least ten times the longest backbone carbon T_1, excluding any possible differential saturation effect. Further, the agreement between ^{13}C and ^1H results show that there can be no significant NOE difference between carbons in different sequences.
(64) F. P. Price, *J. Chem. Phys.*, **36**, 209–218 (1962).
(65) W. Feller, "An Introduction to Probability Theory and its Applications", Vol. 1, Wiley, International Edition, New York, N.Y., 1968.
(66) F. R. Mayo and A. A. Miller, *J. Am. Chem. Soc.*, **80**, 2483 (1958).
(67) M. Litt, *Macromolecules*, **4**, 312–313 (1971).
(68) J. A. Seiner and M. Litt, *Macromolecules*, **4**, 308–311, 314–316, 316–319 (1971).
(69) D. F. Evans, *J. Chem. Soc.*, 345–347 (1953).
(70) No weak resonances were obscured by solvent lines; this was confirmed by recording a spectrum (at 90.52 MHz) in benzene-d_6. Peak positions agreed to within 0.5 ppm, and the higher observing field strength allowed the complete separation of several resonances which appeared as shoulders on the main peaks at 25.16 MHz (specifically those at 137.56, 130.57, 130.04, 126.28, 125.91, and 84.13 ppm).
(71) Mayo has also proposed that the polyperoxides contain an unknown proportion of isolated methylene units in $-OCH_2O-$ sequences.[38] In trioxane–dioxane copolymers, the central methylene carbon in the sequence $OCH_2CH_2OCH_2OCH_2CH_2O$ gives a resonance at 95.97 ppm {D. Fleischer and R. C. Schulz, *Makromol. Chem.*, **176**, 677–689 (1975)}. The only resonance in this region is observed at 92.50 ppm (Figure 4), which is therefore at too high a field to be due to this type of unit.
(72) It might be expected that the end groups, due to their greater motional freedom, would have considerably longer T_1 values than the backbone units and present problems for quantitative analysis in the ^{13}C spectrum due to differential saturation at the pulse interval employed (3.0 s). However, the only resonances to show any appreciable gain in intensity in a spectrum obtained with a 20 s pulse interval were those assigned to benzaldehyde and the carbonyl resonances at 195.04 and 196.12 ppm.
(73) D. Lindsay, J. A. Howard, E. C. Horswill, L. Iton, K. U. Ingold, T. Cobbley, and A. Ll, *Can. J. Chem.*, **51**, 870–880 (1973).
(74) D. Doddrell and A. Allerhand, *J. Am. Chem. Soc.*, **93**, 1558–1559 (1971).
(75) K. F. Kuhlmann, D. M. Grant, and R. K. Harris, *J. Chem. Phys.*, **52**, 3439–3448 (1970).
(76) J. R. Lyerla and G. C. Levy, in ref 1a, pp 79–148.
(77) F. A. L. Anet, in ref 1a, pp 209–227.
(78) M. Nozaki, K. Shimada, and S. Okamoto, *Jpn. J. Appl. Phys.*, **10**, 179–187 (1971).
(79) In the gauche conformation, the β-CH_2 protons make their maximum contribution to the relaxation of C_1, but this can readily be shown to be only about 17% of the total; in the trans conformation, their contribution is only about half as great. In any event, the T_1 of the quaternary carbon is not highly sensitive to the main-chain conformation. The plane of the phenyl ring is assumed to be orthogonal to the $C_\beta C_\alpha C_1$ plane, with approximately tetrahedral backbone angles.

Constrained Anisotropic Motions of Cilia on Crystal Lamellar Surfaces in Polymers

D. C. Douglass,* V. J. McBrierty, and T. A. Weber

Bell Laboratories, Murray Hill, New Jersey 07974. *Received August 3, 1976*

ABSTRACT: A model of flexible polymer chain ends, cilia, characterized by bend and twist between segments, is used to estimate motionally averaged NMR line widths for polyethylene, poly(vinylidene fluoride), and poly(chlorotrifluoroethylene). Comparison with existent data indicates that the model provides a simple format for qualitative discussion of the motion of cilia and loops.

I. Introduction

It is becoming increasingly evident from the interpretation of NMR relaxation data that there are often serious inadequacies in the use of the simple two-phase model[1] to describe a semicrystalline polymer. These conclusions are borne out in morphological studies which support the view that material, characteristic of the crystalline-amorphous boundary region, may be present in sufficient amounts as to constitute a separate macroscopic phase in model calculations.[2–14] This paper is the second in a series which deals with models of molecular motion applicable to molecules in this intermediate region.

The need for such refinements was recognized at an early stage in several studies that demonstrated the need for a third phase in the line shape analysis of broadline spectra from semicrystalline polymers.[15–20] More recently, Fujimoto and co-workers[21] utilized multiple pulse sequences to resolve three components in their T_2 and $T_{1\rho}$* measurements on Nylon and polyethylene which contrasted with the two-component decays usually observed.

Even with two-component T_2 decays there is an implicit need to invoke a third phase in order to arrive at an adequate description of certain features of the longer T_2 temperature curves; we specifically refer to the plateau which occurs at temperatures well in excess of the glass transition temperature T_g. Such behavior, which is typical of several polymers,[22–25] may be rationalized with ease when it is recognized that the longer T_2 in the two-component decay scheme is, in fact, a weighted average of the intermediate and long T_2's in the three-component analysis.

The third phase, identified as the boundaries between crystalline and amorphous regions, contains a preponderance of chain folds and unterminated chain ends or cilia.[2–14] These morphological entities exhibit motional behavior character-

istically different from that experienced by chains in either the crystalline or amorphous regions. The relative magnitudes of the component T_2's in Fujimoto's data[21] show that the degree of motional vigor attained by molecules in the boundary region is intermediate between the near liquid-like character of the the amorphous molecules above T_g and the more restricted motions in the crystalline interior. Similar conclusions result from line shape analyses.[15-20] The fact that the folds and cilia are anchored to the crystalline lamellar surfaces constitutes a limiting constraint upon the motions which are ultimately achieved.

A precise understanding of the nature of fold and cilia behavior is important for many reasons, not least of which stems from the fact that they exert an influence upon the overall relaxation properties of the polymer as, for example, the dielectric or mechanical loss.[24-27] In another context, there is growing conviction that elastomers reinforced with filler particles such as carbon black are in many respects similar to semicrystalline polymers with regard to the molecular configurations and motions experienced by the amorphous molecules. Recent NMR studies on filled rubbers tend to support this conclusion and reasonable interpretations are possible on the assumption that at least some of the rubber molecules can assume fold and cilia configurations on the surface of the filler particles.[28]

An earlier paper has examined the constrained anisotropic motions of folds on the surface of crystal lamella using the wormlike chain as the basis for the model.[29] The predicted T_2 magnitudes were consistent with experimental observations. This paper is concerned exclusively with the construction of a simple model for calculation of the T_2 resulting from motions of cilia. Relevant but more complicated models of cilia, based upon enumeration of configurations on lattice, have been presented by Lax,[30] Meier,[31] and Hesselink.[32]

II. Development of the Model

A typical cilia is considered to be constructed from N connected chain segments. Local coordinate frames are defined for each segment where the polar axis in each case is constrained to lie along the chain axis. XYZ is a crystal coordinate frame in which the XY plane represents the surface of the crystal and the Z direction is perpendicular to the crystal face. In any one of the local frames, say the Nth, a typical internuclear vector is $\mathbf{S}_0$. The coordinates, $\mathbf{S}_N$, of this internuclear vector in the crystal frame are related to $\mathbf{S}_0$ by

$$Y_2^{q_1}(\mathbf{S}_N) = \sum_{q=-2}^{+2} D_{q_1q}^{(2)*}(\Omega_N) Y_2^{q}(\mathbf{S}_0) \qquad (1)$$

where it is convenient, in an NMR context, to work in the spherical harmonic notation.[33] The Euler angles, denoted by Ω_N, bring the crystal frame, XYZ, into coincidence with the Nth local coordinate frame. The symbol $Y_2^q(\mathbf{S})$ denotes the second order spherical harmonic, $(-1)^q[5(2-q)!/4(2+q)!]\cdot P_2^q(\theta)e^{iq\phi}$, where $P_2^m(\theta)$ is the associated Legendre polynomial and θ and ϕ are the polar and azimuthal angles of $\mathbf{S}$. The rotation matrix elements, $D_{q_1q}^{(2)*}(\Omega_N)$, define the linear transformation between spherical harmonics in the crystal and Nth local coordinate frames. The transformation of coordinates defined by eq 1 may be alternatively effected by repeated transformations for successive segments of the cilia. Thus

$$D_{q_1q}^{(2)*}(\Omega_N) = D_{q_1q}^{(2)*}(\omega_N, \omega_{N-1}, \ldots \omega_2, \omega_1) \qquad (2)$$

where, in general, $\omega_k \equiv (\alpha_k, \beta_k, \gamma_k)$ are Euler angles which take the kth frame into coincidence with the $(k+1)$ frame. Equation 2 may be conveniently rewritten

$$D_{q_1q}^{(2)*}(\Omega_N) = \sum_{q_2 \ldots q_N=-2}^{+2} \prod_{j=1}^{N} D_{q_j,q_{j+1}}^{(2)*}(\omega_j) \qquad (3)$$

where $q_{N+1} = q$.

At this point we inject specific character into the model by identifying the Euler angles $(\alpha_j\beta_j\gamma_j)$ to be $(\alpha_j, \beta_j, -\alpha_j + \delta_j)$ as in the earlier analysis on folds.[29] β_j is the angle between successive polar axes and denotes the magnitude of the bend between the respective chain segments. The direction in which the chain bends is determined by α_j; averaging α_j over 2π makes the bend direction random about the preceding polar axis. For succeeding coordinate systems to return as closely as possible to the preceding configuration, that is to achieve minimal twist consistent with the given bend, the third angle γ is $-\alpha_j$; a twist of δ away from this least strained configuration identifies γ as $-\alpha_j + \delta$. The angle δ can assume a distribution of values for the various segments of the cilia. If, however, the same twist angle is used throughout, this approximates a rotation of the chain through δ about a fixed chain axis configuration. Averaging δ over 2π provides complete rotation of the chain. As with all motional averaging the average is performed on eq 1 prior to squaring; we recall that eq 1 is ultimately squared to obtain T_2, the NMR parameter of interest here.

Motions of folds and cilia which are observable in the experimental NMR data occur at temperatures in the region of the glass transition and above. Thus the truly amorphous molecules are in vigorous motion. It is reasonable then to assume that the cilia are also in a state of extensive motion. With this in mind, we consider a model in which each successive element of the chain is rotating about the polar axis of the previous element. This *motional* effect is not to be confused with the element adopting a statistically random direction with respect to the previous element (the latter is effected by performing the average over α after eq 1 is squared).

The motionally averaged expression, obtained by randomizing α in eq 1 over a circle, may be written

$$\overline{Y_2^{q_1}(\mathbf{S}_N)} = \{e^{-iq_1\delta} d_{q_1q_1}^{(2)}(\beta)\}^N Y_2^{q_1}(\mathbf{S}_0) \qquad (4)$$

For β small $\{d_{q_1q_1}^{(2)}(\beta)\}^N$ takes the convenient approximate form

$$\{d_{q_1q_1}^{(2)}(\beta)\}^N \simeq e^{-N[6-q_1^2]\beta^2/4} \qquad (5)$$

Substitution of eq 5 into eq 4 and squaring the resulting expression leads to

$$|Y_2^{q_1}(\mathbf{S}_N)|^2 = e^{-N[6-q_1^2]\beta^2/2} |Y_2^{q_1}(\mathbf{S}_0)|^2 \qquad (6)$$

The use of eq 6 along with established formula[34-36] permits the direct evaluation of T_2 for each element of the cilia. As with earlier calculations, only *intra* contributions within the individual elements are considered. If, in addition to each element rotating about the polar axis of the previous element, the molecule is rotating internally about its own axis, then δ assumes a motional average over a circle in which case $q_1 = 0$ in eq 4 and subsequent expressions.

Equation 6 states simply that the three lattice sums required for the evaluation of T_2 ($q_1 = 0, 1, 2$) are the corresponding *intra* rigid lattice sums multiplied by the exponential factor $\exp(q_1^2 - 6)N\beta_2/2$. In order to compute an overall T_2 for the cilia, a simple average over the array of individual element T_2's is performed. In doing so it is realistic to exclude those elements of the cilia characterised by a T_2 which is within a factor of 2 of the value for element $N = 0$, that is, the first element which is constrained to emerge at right angles from the crystal lamellar surface. The excluded elements are essentially indistinguishable from the crystalline T_2 component in a semicrystalline polymer. Let us suppose that the first m elements are excluded and that a total of P elements are considered. The actual magnitude to be assigned to m will depend upon crystallographic parameters of the polymer under consideration. The average over the $(P-m)$

Table I
Experimental T_2 Data Pertaining to the Intermediate Region

Polymer	Type of sample	Resolved intermediate T_2	Exptl T_2, μs	Ref
PE	Isotropic	No	65	22
	Isotropic	Yes	46	21
PCTFE	Fiber $\gamma' = 0$		100	
	$\gamma' = 54$	No	160	23
	$\gamma' = 90$		150	
PVF_2	Isotropic ^{19}F	No	65	24
	^1H		50	

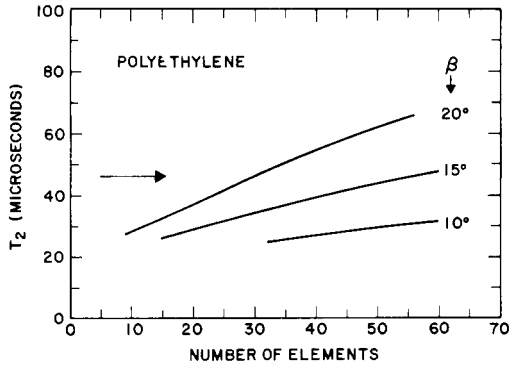

Figure 1. Calculated powder-average, motionally averaged relaxation time, t_2, of ^1H as a function of the number of CH_2 units in the cilia. Chain flexibility is characterized by the bend angle between units, β. Interunit contributions to T_2 are neglected.

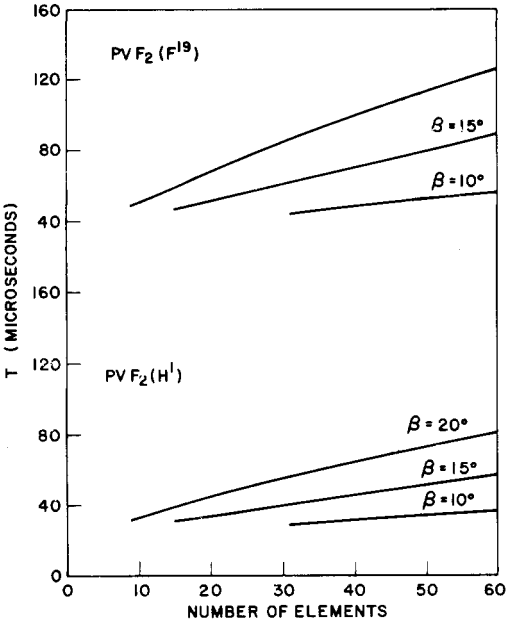

Figure 2. Calculated powder-average, motionally averaged relaxation time, T_2, of ^1H and ^{19}F as a function of the number of CH_2CF_2 units in the cilia. Chain flexibility is characterized by the bend angle between units, β. Interunit contributions to T_2 are neglected.

elements may be performed directly on the preexponential factor as follows.

$$\frac{1}{(P-m)}\sum_{N=m+1}^{P} e^{(q_1^2-6)N\beta^2/2} = e^{(q_1^2-6)(m+1)\beta^2/2}\frac{e^{(q_1^2-6)(P-m)\beta^2/2}-1}{(P-m)\,e^{(q_1^2-6)\beta^2/2}-1} \quad (7)$$

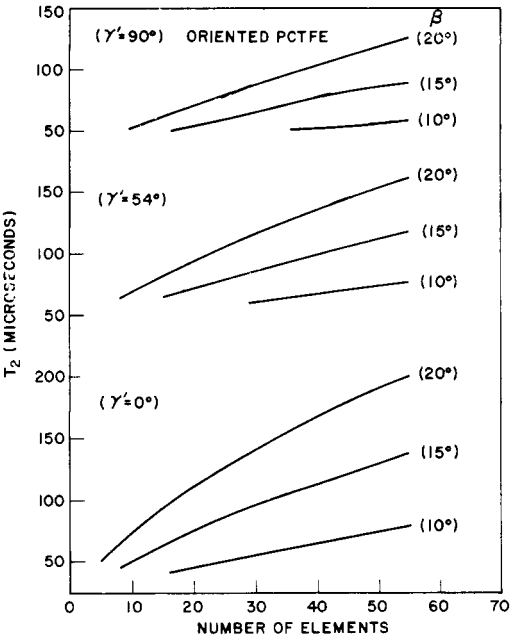

Figure 3. Calculated fiber-average, motionally averaged relaxation time, T_2, ^{19}F as a function of the number of CF_2 units in the cilia for three fiber orientations, $\gamma' = 90$, 54, and 0°, where γ is the angle between fiber axis and magnetic field. Chain flexibility is characterized by the bend angle between unts, β. Interunit contributions to T_2 are neglected.

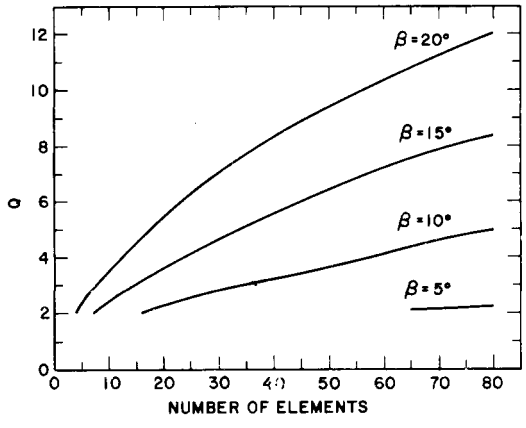

Figure 4. Q, the ratio of the powder-average, motionally averaged relaxation time, T_2, to the rigid-lattice powder-average relaxation time. T_{2RL} as a function of the number of units in the cilia. Interunit contributions to T_2 are neglected. The cilia units are rotating rapidly about the chain axis.

For the internally rotating cilia molecule T_2 for each element takes the form

$$T_2^{-2} = e^{-3N\beta^2}T_{2RL}^{-2} \quad (8)$$

where T_{2RL} is the *intra* rigid lattice T_2. The number of excluded elements may be readily computed to be $(2 \ln 2)/3\beta^2$. Substitution into eq 7 provides the T_2 for the internally rotating cilia and, as a result of the absence of q_1 dependence, T_2 may be written

$$T_2 = \left\{\frac{(P-m)(1-e^{-3\beta^2})}{e^{-3(m+1)\beta^2}(1-e^{-3(P-m)\beta^2})}\right\}^{1/2} T_{2RL} = Q \cdot T_{2RL} \quad (9)$$

P denotes the total number of elements considered and $m \simeq (2 \ln 2)/3\beta^2$, the number of excluded elements.

Table II
Comparison of Data and Model T_2 for PCTFE

Fiber orientation angle, γ', deg	Exptl noncrystalline T_2, μs	Exptl T_2 assigned to cilia,[a] μs	T_{2RL}, μs	Q	Calcd noncrystalline T_2, μs
0	100	49	20.4	2.4	122
54	160	102	29.3	3.5	153
90	150	91	23.9	3.8	136

[a] See text.

III. Comparison with Experiment

The theory outlined above may be applied to three polymers for which adequate experimental data are available: branched polyethylene (PE),[22] poly(chlorotrifluoroethylene) fibers (PCTFE),[23] and poly(vinylidene fluoride) (PVF_2).[24] The relevant experimental data are summarized in Table I. The T_2 component assigned to the intermediate lamellar surface region is unresolved from the highly mobile amorphous signal in all cases with the exception of the PE data of Fujimoto et al.[21] Consequently, we shall have to make plausible assignments of T_2 magnitudes to the amorphous T_2 in order to check whether or not the motions available to the cilia are sufficient to account for the observed plateau. This of course does not infer that the plateau is due to cilia alone but rather that they have the capability, as already demonstrated in the case of folds,[29] of providing T_2's of the correct order of magnitude.

Equations 6 and 7 have been used along with the usual expression for T_2 to compute an average T_2 for the nonrotating cilia. The results for the three polymers are plotted for bend angles β = 10, 15, and 20° in Figures 1–3. Figure 4 displays the dependence of Q, the factor required in the computation of T_2 for the rotating cilia, upon the total number of elements, P, for the same three bend angles.

It is immediately apparent from Figure 1 that the model can comfortably accommodate a T_2 of 46 μs as observed in PE.[21] Typically, about 30 elements and a bend angle of 20° will provide an adequate description of the experimental observations. For rotating cilia, some 12 elements are required for the same bend angle as deduced from Figure 4 on the basis of T_{2RL} = 12.2 μs. The weighted T_2 of 65 μs for the intermediate and amorphous regions observed by McCall and Falcone[22] is consistent with the results of Fujimoto et al.[21] which provide an amorphous T_{2a} = 200 μs of about the same intensity as the T_2 from the intermediate region.

The overall relaxation behavior of branched PE would tend to indicate that rotating cilia are more probable.[25] The γ_c relaxation is fully active in the plateau temperature region (~50 °C). In addition, this is precisely the temperature at which the $\alpha_c T_{1\rho}$ minimum occurs[22] (We recall that $T_{1\rho}$ corresponds roughly to the same correlation frequencies as T_2). Both relaxations have been interpreted in terms of chain rotation.[25]

We now turn our attention to PVF_2 for which the T_2 plateau magnitudes are $T_2(^1H)$ = 50 μs and $T_2(^{19}F)$ = 65 μs for proton and fluorine resonance, respectively.[24] These magnitudes represent the weighted T_2 for the intermediate surface regions (40%) and amorphous regions (60%). Proceeding on the basis of the reasonable assumption of T_{2a} = 200 μs, the average cilia T_2's required to achieve agreement with experiment are 32.2 and 42.5 μs for proton and fluorine resonance, respectively. The corresponding rigid lattice T_2's are $T_2(^1H)_{RL}$ = 15 μs and $T_2(^{19}F)_{RL}$ = 20.4 μs.[24] It is evident that far fewer elements are required for any given angle β as compared with PE for either rotating or nonrotating cilia. Alternatively stated, a smaller bend angle is predicted for an equivalent number of elements. This is consistent with the expectation that the PVF_2 chain is much less flexible than the PE chain.

The theoretical predictions for the nonrotating PCTFE cilia are especially interesting in a fundamental respect: the anisotropy in T_2 as a function of angle is at odds with experimental observation of a maximum in T_2 at an orientation angle μ' = 54°. This would tend to rule out nonrotating cilia, a conclusion in agreement with earlier interpretation.[29] The data pertaining to rotating cilia are summarized in Table II wherein theoretical predictions are compared with experimental data. As with the earlier calculation on folds,[29] an amorphous T_2 of 200 μs is assumed and the intermediate region comprises 20% of the noncrystalline material present. In calculating the overall T_2 noncrystalline component (cilia plus amorphous) a mean Q of 3.2 has been used. The results indicate that the model experiences difficulty in developing sufficient anisotropy in T_2 as a function of orientation angle γ'. Indeed a much better fit can be achieved at higher temperatures (~160°) where $T_2(\gamma' = 0)$ rapidly approaches $T_2(\gamma' = 54°, 90)$. Thus one must turn to another feature, such as folds, in order to adequately account for the PCTFE data.

References and Notes

(1) C. W. Wilson and G. E. Pake, *J. Polym. Sci.*, **10**, 503 (1953).
(2) Von H. G. Zachmann, *Kolloid Z. Z. Polym*, **216**, 180 (1967).
(3) A. Keller and D. J. Priest, *J. Macromol. Sci., Phys.*, **2**, 479 (1968).
(4) M. I. Bank and S. Krimm, *Bull. Am. Phys. Soc.*, **14**, 442 (1969).
(5) J. M. Stellman and A. E. Woodward, *Polym. Lett.*, **7**, 755 (1969).
(6) R.-J. Roe and H. E. Bair, *Macromolecules*, **3**, 454 (1970).
(7) R.-J. Roe, *J. Chem. Phys.*, **53**, 3026 (1970).
(8) A. Peterlin, H. G. Olf, W. L. Peticolas, G. W. Hibler, and J. L. Lippert, *Polym. Lett.*, **9**, 583 (1971).
(9) A. Peterlin and G. Meinel, *J. Polym. Sci., Part B*, **3**, 1059 (1965).
(10) E. W. Fischer and G. Schmidt, *Angew. Chem.*, **74**, 551 (1962).
(11) A. Keller, E. Martuscelli, D. J. Priest, and Y. Udagawa, *J. Polym. Sci., A*, **2**, 1807 (1971).
(12) F. J. B. Calleja and D. R. Rueda, *Polym. J.*, **6**, 216 (1974).
(13) V. Petraccone, I. C. Sanchez, and R. S. Stein, *Polym. Prepr., Am. Chem. Soc., Div. Polym. Chem.*, **15**, 485 (1974).
(14) K. Nakagawa and Y. Ishida, *J. Polym. Sci. Polym. Phys. Ed.*, **11**, 2153 (1973).
(15) K. Bergmann and K. Nawotki, *Kolloid Z. Z. Polym.*, **219**, 132 (1967).
(16) K. Bergmann, *Kolloid Z. Z. Polym.*, **251**, 962 (1973).
(17) W. Piesczek and E. W. Fischer, *IUPAC Macromol. Symp. Prepr., Leiden*, **13**, 873 (1970).
(18) B. Schneider, H. Pivcova, and D. Diskocilova, *Macromolecules*, **5**, 120 (1972).
(19) J. B. Smith, A. J. Manuel, and I. M. Ward, *Polymer*, **16**, 57 (1975).
(20) J. Loboda-Cackovic, R. Hosemann, and W. Wilke, *Kolloid Z. Z. Polym.*, **235**, 1253 (1969).
(21) K. Fujimoto, T. Nishi, and R. Kado, *Polym. J.*, **3**, 448 (1972).
(22) D. W. McCall and D. R. Falcone, *Trans. Faraday Soc.*, **66**, 262 (1970).
(23) V. J. McBrierty, D. W. McCall, and D. C. Douglass, *Bull. Am. Phys. Soc.*, **15**, 307 (1970).
(24) V. J. McBrierty, D. C. Douglass, and T. A. Weber, *J. Polym. Sci., Polym. Phys. Ed.*, submitted.
(25) V. J. McBrierty and I. R. McDonald, *Polymer*, **16**, 125 (1975).
(26) J. D. Hoffman, G. Williams, and E. Passaglia, "Transitions and Relaxations in Polymers", R. F. Boyer, Ed., Interscience, New York, N.Y., 1966 p 173.
(27) K. Nakagawa and Y. Ishida, *J. Polym. Sci., Polym. Phys. Ed.*, **11**, 1503 (1973).
(28) J. O'Brien, E. Cashell, G. E. Wardell, and V. J. McBrierty, to be published.
(29) D. C. Douglass, V. J. McBrierty, and T. A. Weber, *J. Chem. Phys.*, in press.

See also, V. P. Schmedding and H. G. Zachmann, *Kolloid Z. Z. Polym.*, **250**, 1105 (1972).
(30) M. Lax, *Macromolecules*, **8**, 947 (1975).
(31) D. J. Meier, *J. Phys. Chem.*, **71**, 1861 (1967).
(32) F. Th. Hesselink, *J. Phys. Chem.*, **10**, 3488 (1969).
(33) The convention used for the matrix elements follows that used by M. E. Rose as described in A. A. Wolf, *Am. J. Phys.*, **37**, 531 (1969). Additional sources on this subject are: D. M. Brink and G. R. Satchler, Angular Momentum, 2d ed, Clarendon Press, New York, N.Y., 1968; A. R. Edmonds, Angular Momentum in Quantum Mechanics, Princeton University Press, Princeton, N.J., 1960.
(34) V. J. McBrierty and D. C. Douglass, *J. Magn. Reson.*, **2**, 352 (1970).
(35) J. H. Van Vleck, *Phys. Rev.*, **74**, 1168 (1948).
(36) V. J. McBrierty, *Polymer*, **15**, 503 (1974).

Aggregation of Poly(*n*-hexyl isocyanate) in Toluene. A Dielectric and Electric Birefringence Study

H. J. Coles,* A. K. Gupta, and E. Marchal

Centre de Recherches sur les Macromolécules, CNRS, 67083 Strasbourg, France.
Received June 7, 1976

ABSTRACT: Measurements have been made by dielectric relaxation and electric field birefringence on poly(*n*-hexyl isocyanate)–toluene solutions. Four molecular weights in the range 62 000 to 290 000 have been studied over a wide concentration range. The results by the two methods are in good accord and suggest the existence of both linear head-to-tail and antiparallel side-by-side aggregation for the low molecular weight samples and only antiparallel side-by-side aggregation for the high molecular weight samples. The relative amounts of aggregation have been shown to be concentration and temperature dependant.

The solution properties of poly(alkyl isocyanates) have attracted much interest recently because of their apparent helical conformation and high chain stiffness. Of these isocyanates both the highly polar *n*-butyl isocyanate (PBIC) and *n*-hexyl isocyanate (PHIC) have been studied in various solvents by light scattering,[1,2] viscosity,[3-5] infrared spectroscopy,[6] electric birefringence,[7,8] and dielectric relaxation methods.[9-11] It has been shown by several authors that both these polymers can be described by a wormlike chain model.

It is generally concluded that aggregation does not occur with these systems. However, this conclusion appears to have been made for measurements with nonpolar solvents over a restricted concentration range or for polar solvents. While it is well known that highly polar polypeptide (helical and rod-like) molecules do not generally form aggregates in polar solvents they do so in nonpolar solvents.[12-15] It is therefore perhaps surprising that the isocyanates with similar characteristics do not show the same behavior in nonpolar solvents.

We have chosen to examine this behavior in well fractionated PHIC samples in toluene solutions. Measurements were made by dielectric relaxation and electric field birefringence, both methods being sensitive to structural changes, over a large concentration range. For these solutions temperature dependence studies were also made. The results clearly indicate the existence of aggregation in these solutions and further, we believe, explain the discontinuities recently recorded in temperature dependence studies.[16,17] Finally we compare salient characteristics of the current results with those obtained with polypeptides in nonpolar solvents.[18]

Experimental Section

The PHIC samples were kindly donated by J. Pierre of Professor Desreux's group at Liège University. They were prepared according to the method described by Shashoua[19] and fractionated by precipitation using the carbon tetrachloride–methanol system. Their weight average molecular weights determined by light scattering in chloroform were 62 000, 90 000, 140 000 and 290 000, and these samples will be denoted PHIC (62 000), PHIC (90 000), PHIC (140 000) and PHIC (290 000), respectively. The ratio of the weight to the number average molecular weight as determined by gel permeation chromatography in tetrahydrofuran (THF) at 25 °C was less than 1.2, indicating a low polydispersity.

Solutions were made up with freshly distilled toluene on a gravimetric basis, and measurements were made at room temperature of 23.0 ± 0.5 °C, unless otherwise stated.

The dielectric absorption measurements, in the range 20 Hz to 2 MHz, were made on the two impedance bridges described previously[20] and a General Radio 1616 bridge. Two stainless steel cylindrical cells of air capacitance 13 and 196 pF were used. They were enclosed in a thermostatically controlled chamber which maintained their temperature to within ±0.1 °C.

The birefringence measurements were made by the pulsed dc field method. The sample cell (length 7.5 cm) was placed between crossed Glan-Thomson polarizers with the applied field at 45° to the polarizer azimuth. The system was such that the beam of the low powered He–Ne laser (λ 633 nm) probed the field induced birefringence which was recorded as an intensity change via a red sensitive photomultiplier–storage oscilloscope system. The pulsed dc field was from 0 to 2.5 kV cm^{-1} and of duration variable from 10 μs to 10 ms. This apparatus which included novel features in the cell design will be described in greater detail elsewhere.[21]

Theory

Macromolecules in solution are free to orientate, being on average randomly oriented in the absence of an applied field. If these molecules are polar they tend to align under the application of an electric field. In this situation the polarizability produced is measured through the dielectric constant, and the induced or inherent optical anisotropy is manifest through the induced birefringence. Both the dielectric and the birefringence techniques give information on dipole moments and rotational relaxation times and both have been used in the present work. Each method has its advantages. At low frequencies of applied field we measure the dielectric constant ϵ_0, at high frequencies, where the dipoles have insufficient time to obtain an equilibrium distribution at each stage of the alternating cycle, we measure ϵ_∞. The dielectric increment $\Delta\epsilon = \epsilon_0 - \epsilon_\infty$ is related to the mean-square dipole moment $\overline{\mu^2}$ by the following:

$$\frac{\overline{\mu^2}}{M} = \frac{9kT}{4\pi N_A} \frac{(2\epsilon^2 + n^4)}{\epsilon^2(n^2+2)^2 d} \frac{\Delta\epsilon}{w} \quad (1)$$

* Address correspondence to this author at the Physics Department, Brunel University, Uxbridge, Middx, UB39H, U.K.